Structural and Optical Properties of $BaMgAl_{10}O_{17}:Eu^{2+}$ Phosphor

Kwang-Bok Kim,*,† Yong-Il Kim,‡ Hui-Gon Chun,§ Tong-Yul Cho,§ Jae-Sun Jung,|| and Jun-Gill Kang*,||

Electronics and Telecommunications Research Institute, P.O. Box 106, Yuseong, Daejeon 305-350, Korea, Korea Research Institute of Standards and Science, P.O. Box 102, Yuseong, Daejon 305-600, Korea, School of Materials Science and Engineering, University of Ulsan, Ulsan 609-735, Korea, and Department of Chemistry, Chungnam National University, Daejeon 305-764, Korea

Received May 21, 2002. Revised Manuscript Received September 4, 2002

$BaMgAl_{10}O_{17}:Eu^{2+}$ phosphors are synthesized by solid-state calcining of $BaCO_3$, Al_2O_3, MgO, and Eu_2O_3 with AlF_3 as a flux. The structural and optical properties of the blue phosphor are investigated as a function of the europium concentration in $BaMgAl_{10}O_{17}$ using the neutron and the X-ray powder diffraction methods and luminescence and X-ray absorption near-edge structure (XANES) spectroscopies. The unit cell parameters of $BaMgAl_{10}O_{17}:Eu^{2+}$ blue phosphor are calculated through the Rietveld refinements of the X-ray and neutron diffraction data. In addition, the maximum electron energy density of the phosphor is calculated using the maximum entropy method to reveal the overall structural changes in $BaMgAl_{10}O_{17}$ and $BaMgAl_{10}O_{17}:Eu^{2+}$. The critical concentration is estimated from the concentration dependencies of the absolute quantum efficiency and the intensity of the photoluminescence. The XANES spectrum reveals that nonsubstituted Eu ions exist in the trivalent state above the critical concentration.

1. Introduction

Eu^{2+}-doped barium magnesium aluminate, or $BaMgAl_{10}O_{17}:Eu^{2+}$ (BAM), is a blue-emitting phosphor that is of great interest for use in plasma display panel (PDP).[1] The characteristic feature of the blue luminescence can be coordinated with a strong crystal-field strength and a high degree of covalency of the host lattice and the allowed 5d → 4f transition of Eu^{2+}. The intensity of BAM emission decreases markedly when there is excessive Eu^{2+} ion doping. The concentration that quenches the emission from BAM could be due to energy transfer between the Eu^{2+} ions, which is closely related to the crystal structure in BAM phosphor.[2,3] Most studies of the quenching concentration have focused on the quantitative chemical analysis of the amount of Eu^{2+} in the starting mixture. However, it is very important to determine the critical concentration of Eu^{2+} in the crystal lattice since the amount of doped Eu^{2+} is directly related to the concentration quenching and the degradation mechanism in BAM. The critical distance for energy transfer of Eu^{2+} is a very important factor for understanding the $Eu^{2+}-Eu^{2+}$ energy transfer mechanism. In general, the critical distance for energy transfer has been evaluated from the overlap of the excitation and the emission spectra according to Dexter's equation.[4] However, it is very difficult to calculate the critical distance of Eu^{2+} exactly using the absorption, excitation, and emission spectra in BAM. Detailed information on the crystal parameters of BAM is very important for understanding the underlying mechanism of its luminescence property. However, the precise location of Eu^{2+} is not known yet. The structure of $BaMgAl_{10}O_{17}$, or β-alumina, consists of two spinel blocks ($MgAl_{10}O_{16}$) separated by one mirror plane (BaO), as shown in Figure 1.[5−7] When Eu^{2+} is substituted into the host lattice, it can have three possible locations: Beevers-Ross (BR), anti-Beevers-Ross(a-BR), and mid-oxygen (mO) sites in the mirror plane. Single-crystal X-ray diffraction of Eu^{2+} and Eu^{3+} ions in related β''-alumina has shown that the majority of Eu ions occupy mO sites in both cases.[8] Recently, nuclear quadrupole calculation has shown that an a-BR site is energetically more stable than the other two sites.[9]

This work characterized the structural and optical properties as a function of the Eu^{2+} concentration in BAM. To determine the structural properties, we col-

* To whom correspondence should be addressed. K.-B. Kim: phone, +82-42-860-6251; fax, +82-42-860-5202; e-mail, kkb63422@etri.re.kr. J.-G. Kang: phone, +82-42-821-6548; fax, +82-42-823-1360; e-mail, jgkang@cnu.ac.kr.
† Electronics and Telecommunications Research Institute.
‡ Korea Research Institute of Standards and Science.
§ University of Ulsan.
|| Chungnam National University.

(1) Yocom, N.; Meltzer, R. S.; Jang, K. W.; Grimm, M. 1st International Conference *On the Science and Technology of Display Phosphors*, San Diego, CA, 27, 1995.
(2) Kutty, T. R. N.; Nayak, M. *Mater. Chem. Phys.* **2000**, *65*, 158.
(3) Liu, Y.-L.; Shi, C.-S. *Mater. Res. Bull.* **2001**, *36*, 109.
(4) Dexter, D. L. *J. Chem. Phys.* **1953**, *21*, 836.
(5) Kimura, S.; Bannai, E.; Shindo, I. *Mater. Res. Bull.* **1982**, *17*, 209.
(6) Iyi, N.; Takekawa, S.; Bando, Y.; Kimura, S. *J. Solid State Chem.* **1983**, *47*, 34.
(7) Iyi, N.; Inoue, Z.; Takekawa, S.; Kimura, S. *J. Solid State Chem.* **1984**, *52*, 66.
(8) Carrilo-Caberra, W.; Thomas, J. O.; Farrington, G. C. *Solid State Ionics* **1986**, *18&19*, 645.
(9) Stephan, M.; Schmidt, P. C.; Mishra, K. C.; Raukas, M.; Ellens, A.; Boolchand, P. *Z. Phys. Chem.* **2001**, *215*, 1397.

10.1021/cm020592f CCC: $22.00
Published on Web 11/13/2002

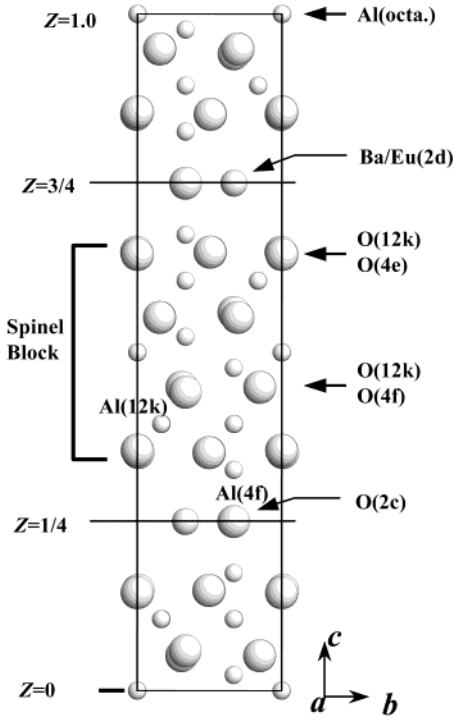

Figure 1. Projection of unit cells of $BaMgAl_{10}O_{17}$ β-alumina crystal structure on the [1$\bar{1}$0] plane.

lected X-ray and neutron powder diffraction data for BAM. Structural information on BAM was obtained by analyzing the diffraction data using the Rietveld refinement method. In addition, we applied the maximum entropy method (MEM) to obtain further structural information from diffraction data independently of a structure model.[10−12] It has been proven that there is a large advantage to combining these methods.[13] Information on the surrounding atoms can be obtained from a Fourier map generated from the phase of the structure factors calculated for the best model and their observed intensities. Usually, MEM requires knowledge of the phase of the Bragg reflections, as obtained from refinement. When the individual intensities can be determined for a sufficient number of reflections, the MEM can also be applied to powder diffraction data. By combining the Rietveld refinement method and the MEM, we obtained structural information on BAM and determined the amount of Eu^{2+} ions in BAM. Information on the crystal structure of BAM allowed us to calculate the critical distance and energy-transfer probability of Eu^{2+} in BAM. To examine the optical properties of BAM, we obtained luminescence and excitation spectra, and X-ray absorption near edge structure (XANES) spectra, and measured the decay kinetics of the luminescence. We also evaluated the absolute quantum efficiency of the photoluminescence. This paper reveals the relationship between the structural arrangement and the concentration of the Eu dopant in quenching the luminescence of BAM.

2. Experimental Section

Preparation and Composition Analysis. Several different BAM phosphors were prepared from the mixture of $BaCO_3$, MgO, α-Al_2O_3, and Eu_2O_3 by varying the ratio of each compound. To control the particle size of BAM in the range of 4−8 μm, 0.010 mol of AlF_3 was added as a flux. All the materials used were of analytical grade exceeding 99.9% purity. The well-mixed mixture was baked at 1400−1420 °C in a H_2(6%) + N_2(94%) atmosphere for 1 h. The baked sample was thoroughly ground and baked again in the same manner. Then, the product was crushed in a ball-mill and washed several times with deionized water. After drying at 120 °C for 48 h, the powder was sieved through a 325 mesh. Chemical analysis of the final product was carried out with a Jovin-Yvon Plasma Trace 1 ICP-AES and a Perkin-Elmer 4100PC AAS. The composition of the europium element in the final products ranged from 0.023 to 0.425 mol/mol of host.

X-ray and Neutron Data Collection and Refinement. The X-ray diffraction data were measured at room temperature in the scattering range of 15°−140° with a 0.04° interval in 2θ using Cu Kα radiation with a graphite monochromator. Furthermore, neutron powder diffraction data were collected up to $2\theta = 140°$ with a 0.05° step/10 s at a neutron wavelength of 1.8348 Å on the High-Resolution Powder Diffractometer (HRPD) at the Hanaro Center, Korea Atomic Energy Research Institute. Structure refinement was carried out by the Rietveld method, using the RIETAN profile refinement program.[14] Of the four profile shape functions in RIETAN, a pseudo-Voigt function was used as the profile function for X-ray and neutron powder diffraction data. This function is very successful for describing the reflection asymmetry due to axial divergence.[15,16] The March-Dollase correction was applied for the preferred orientation effects.[17] The neutron scattering lengths of Ba, Mg, Al, and O atoms are 0.5070, 0.5375, 0.3449, and 0.5803 × 10^{-12}, respectively. In addition, maximum electron energy density (MEED) was calculated, using the maximum entropy method (MEM) program.[18] The MEED program adapts a single constraint, incorporated into the optimization process by a single Lagrange undetermined multiplier λ.[9,18] A value of $\lambda = 0.0001$ was found suitable for all the calculations in this study. The constraint of the form $C = 0$ has two types of contributions. One is the F-type constraint, which originates from the reflections with known phases, and the other is the G constraint, which incorporates overlapping reflections.[18] In the MEM analysis, the unit cell was divided into 64 × 64 × 128 pixels and the final reliable R factors of MEM electron density defined by

$$R_F = \sqrt{\frac{\sum |F_o - F_{MEM}|}{\sum |F_o|}}$$

$$wR_F = \sqrt{\frac{\sum \frac{1}{\sigma^2} |F_o - F_{MEM}|}{\sum \frac{1}{\sigma^2} |F_o|}}$$

where F_{MEM} is a structure factor estimated by the MEM analysis and the summation is carried out over the reflections analyzed by the MEM.

Optical Measurement. The emission spectrum of BAM excited at 254 nm was recorded on an EG&G Spectra-C11. For the excitation spectrum, a deuterium lamp was used as the light source. For the PL spectrum, the sample was

(10) Sakata, M.; Sato, M. *Acta Crystallogr., Sect. A: Found. Crystallogr.* **1990**, *46*, 263.
(11) Sakata, M.; Takata, M. *High-Pressure Res.* **1996**, *14*, 327.
(12) Gilmore, C. J. *Acta Crystallogr., Sect. A: Found. Crystallogr.* **1996**, *52*, 561.
(13) Takta, M.; Umeda, B.; Nishibori, E.; Sakata, M.; Saito, M.; Ohno, Y.; Shinohara, H. *Nature (London)* **1995**, *377*, 46.
(14) Izumi, F.; Ikeda, T. *Mater. Sci. Forum* **2000**, *321−324*, 198.
(15) Thompson, P.; Cox, D. E.; Hasting, J. B. *J. Appl. Crystallogr.* **1987**, *20*, 79.
(16) Finger, L. W.; Cox, D. E.; Jephcoat, A. P. *J. Appl. Crystallogr.* **1994**, *27*, 892.
(17) Dollase, W. A. *J. Appl. Crystallogr.* **1986**, *19*, 267.
(18) Kumajawa, S.; Kubota, Y.; Takata, M.; Sakata, M.; Ishibashi, Y. *J. Appl. Crystallogr.* **1993**, *26*, 453.

irradiated with an He−Cd 325-nm laser line and the spectrum was measured at a 90° angle with an ARC 0.5-m Czerny-Turner monochromator equipped with a cooled Hamamatsu R-933−14 PM tube. For the decay time measurement, we employed a time-correlated single-photon counting system with an Edinburg FL 900 spectrophotometer.

The quantum yield, defined by

$$Q = \frac{\text{number of photons emitted}}{\text{number of photons absorbed}}$$

was measured with a custom-built integrating sphere, manufactured by Lapshere. The 10-cm-diameter sphere is a hollow sphere and coated on the inside with diffusely reflecting materials. The 325-nm laser beam was near normally directed into the sphere through a small entrance hole at the equator, but the beam reflected from the sample surface or the inside wall of the sphere was not allowed to escape via the entrance hole. A diffusely reflecting baffle was positioned between the sample and the exit port to protect from direct illumination. The output of the sphere was directed into an ARC 0.5-m Czerny-Turner monochromator equipped with a cooled Hamamatsu R-933-14 PM tube. The recorded spectra were corrected for the spectral response of the system using an Oriel 45-W quartz tungsten halogen lamp standard. For accurate quantum yield, three measurements were made: measurements of an empty sample holder, a directly excited sample, and an indirectly excited sample. The spectral areas over the excitation and emission wavelength regions (L and P, respectively) are proportional to the numbers of excited and emitted photons, respectively. We calculated the absorption coefficient, A, defined as

$$A = \left(1 - \frac{L_c}{L_b}\right)$$

where L_b and L_c are the spectral areas for the second and third measurements, respectively. The number of absorbed photons is proportional to A times the spectral area, L_a, of the first measurement. To correct for the emission induced indirectly from the reflected excitation beam, the quantum yield can be expressed by

$$Q = \frac{P_c - (1 - A)P_b}{L_a A}$$

where P_b and P_c are the spectral areas under the emission profiles for the second and third measurements, respectively. All measurements were repeated three times. The experimental details were published elsewhere.[19]

3. Results and Discussion

Crystal Parameters and Electron Density. The X-ray and neutron powder diffraction data were collected for BAM blue phosphors with different Eu concentration. The X-ray and neutron powder diffraction patterns show that all the samples have the space group of $P6_3/mmc$, which is consistent with other reports.[17,20] In this work, the structure of $Ba_{0.75}Al_{10}O_{17.25}$ with space group $P6_3/mmc$ was taken as the starting model for synthetic $BaMgAl_{10}O_{17}:Eu^{2+}$ blue phosphor. The neutron diffraction data of the $BaMgAl_{10}O_{17}$ host lattice was initially refined using a unit-cell parameter, the zero-point shift, the displacement factor, and the background parameters since the neutron diffraction is more sensitive to atomic positions and the occupation factors of Al, Mg, and O atoms than is X-ray diffraction. When $(Na, Al)^{4+}$ are replaced by $(Ba, Mg)^{4+}$ in sodium β-alumina, Ba atoms only occupy the 2d position of the mirror plane. Mg atoms, however, may partially occupy either tetrahedral or octahedral sites of Al atoms in the spinel block to achieve charge compensation of $BaMgAl_{10}O_{17}$ compound. It has been proposed that $BaMgAl_{10}O_{17}:Eu^{2+}$ produces a blue luminescence band when Al atoms occupying the tetrahedral site of spinel block are partially replaced by Mg atoms.[21−23] Initially, the Rietveld refinement of the neutron diffraction data for $BaMgAl_{10}O_{17}$ was performed to determine the site preference of Mg atoms for the tetrahedral (T) or octahedral (O) sites. The final weighted R factors, R_{wp}'s, for T and O models are 4.65 and 5.15%, respectively. These results indicate that the Mg atoms preferentially occupy the tetrahedral site, 4f ($^1/_3$, $^2/_3$, z), in the spinel block. The observed and the simulated neutron diffraction data of $BaMgAl_{10}O_{17}$ are shown in Figure 2.

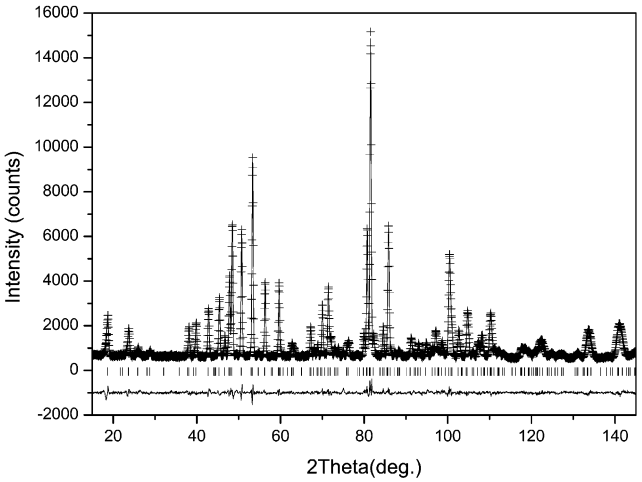

Figure 2. Observed and simulated neutron diffraction patterns of undoped $BaMgAl_{10}O_{17}$. The + symbol and solid line represent the observed and calculated intensities, respectively. The vertical bars represent the reflection position markers, and the differences between the observed and calculated intensities are shown under the vertical bars.

Next, we carried out the Rietveld refinement on the neutron powder diffraction data of $BaMgAl_{10}O_{17}$ doped with europium using the structural model based on the above results and the following two constraints: the total occupancies of the Mg and Al sites and the Ba and Eu sites are unity, and the isotropic atomic displacement parameters of the Mg and Al sites are equal. Using the structural parameters (e.g., lattice parameters, atomic coordinates, isotropic thermal parameters, the occupancy of Mg and Al atomic sites, etc.) obtained from the Rietveld refinement of the neutron powder diffraction data as initial parameters, we continued to refine the X-ray powder diffraction data. Figure 3 shows the observed and the simulated diffraction patterns. The final R_{wp} factors for the neutron and X-ray data were 4.82 and 12.02%, respectively. In BAM containing 11.6 mol % Eu, there was no evidence for other phases except the $BaMgAl_{10}O_{17}:Eu^{2+}$ phase. Any secondary phases,

(19) de Mello, J. C.; Wittmann, H. F.; Friend, R. H. *Adv. Mater.* **1997**, *9*, 230.
(20) Oshima, S.; Kitamura, K.; Shigeta, T.; Horii, S.; Matsuoka, T.; Tanaka, S.; Kobayashi, H. *J. Electrochem. Soc.* **1999**, *146*, 392.
(21) Stevels, A. L. N. *J. Lumin.* **1978**, *17*, 121.
(22) Collin, G.; Comes, R.; Boilpt, J. P.; Colomban, Ph. *Solid State Ionics* **1980**, *1*, 59.
(23) Sommerdijk, J. L.; Stevels, A. L. N. *Philips Tech. Rev.* **1977**, *37*, 221.

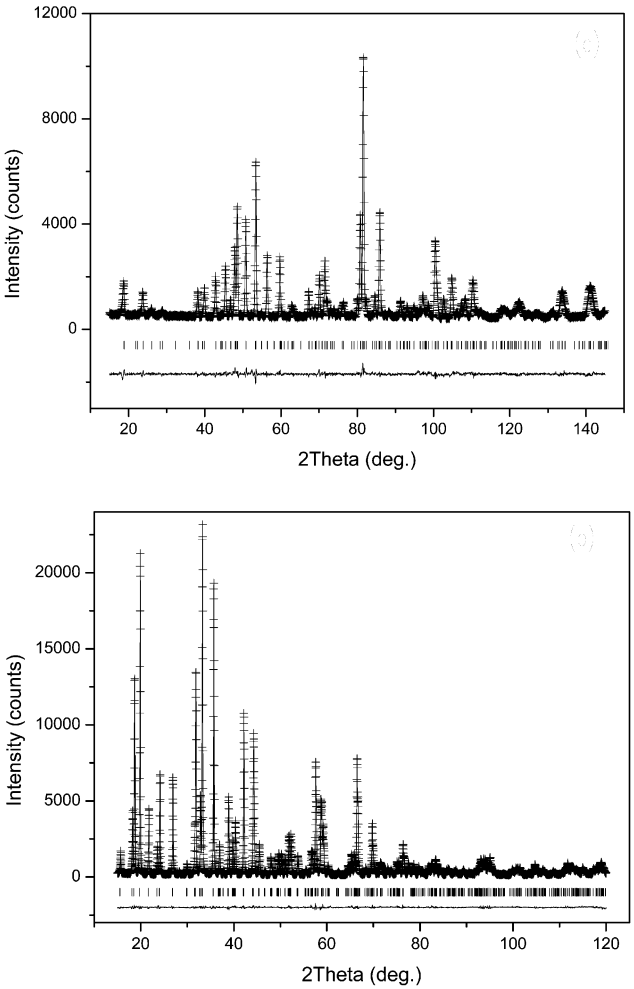

Figure 3. Observed and simulated neutron (a) and X-ray (b) diffraction patterns of $BaMgAl_{10}O_{17}$ doped with 11.6 mol % Eu. The + symbol and solid line represent the observed and calculated intensities, respectively. The vertical bars represent the reflection position markers, and the differences between the observed and calculated intensities are shown under the vertical bars.

such as $BaAl_2O_4$, $BaAl_2O_4$:Eu^{2+}, and $BaAl_{32/3}O_{17}$:Eu^{2+}, were not found. Previously, the last two phosphors were reported to be responsible for the green emission.[21,24]

Finally, simulations of both the neutron and X-ray diffraction patterns of $BaMgAl_{10}O_{17}$:Eu^{2+} were performed for three possible positions of Eu^{2+}: the a-BR position at (0, 0, $^1/_4$), BR at the 2d site ($^1/_3$, $^2/_3$, $^3/_4$), and mO at ($^5/_6$, $^1/_6$, $^1/_4$). There is no difference in the neutron patterns for different Eu^{2+} concentrations because of the large absorption effect of the heavy Eu atom on neutron radiation. This implies that it is very difficult to distinguish Eu sites using neutron powder diffraction data. By contrast, the simulated X-ray powder diffraction patterns are very sensitive to the amounts of Eu atoms. As the Eu atom content increases, the intensity of the peak at $2\theta = 33°$ decreases, while the intensity of the peak at $2\theta = 36°$ increases. Moreover, with increasing Eu atom content, the tiny peak in the range of 2θ from 36° to 37° splits into two peaks. The theoretical X-ray powder diffraction pattern of the BR

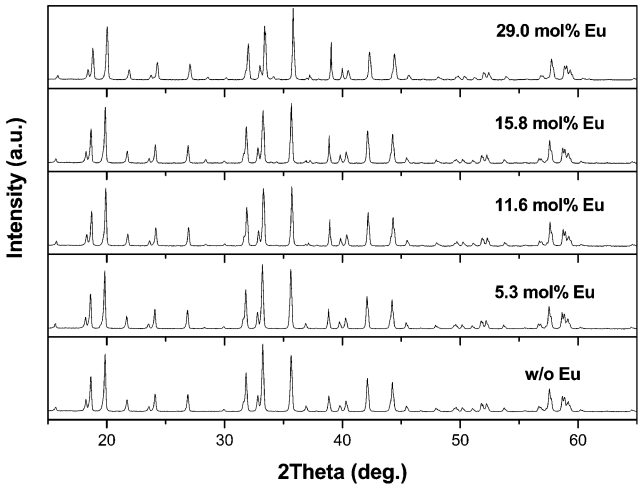

Figure 4. Simulated X-ray diffraction pattern of $BaMgAl_{10}O_{17}$:Eu^{2+} as a function of dopant concentration.

model, shown in Figure 4, is very close to the observed X-ray powder diffraction pattern of $BaMgAl_{10}O_{17}$:Eu^{2+}. For BAM doped with 11.6 mol % Eu, the final respective R_{wp} values of the neutron and X-ray diffraction patterns are 11.31 and 19.05% for a-BR, and 5.05 and 11.29% for BR. The neutron and X-ray diffraction patters could not be refined for the mO site.

For all samples studied in this work, the final R_{wp} for the a-BR model is higher than that for the BR model. Accordingly, we assumed that Eu atoms partially replace Ba atoms occupying the 2d site ($^1/_3$, $^2/_3$, $^3/_4$) on the mirror plane of $BaMgAl_{10}O_{17}$:Eu^{2+}, as suggested previously.[21,23,25] The refined structural parameters and selected atomic distances and bond angles for $BaMgAl_{10}O_{17}$:Eu^{2+} are listed in Tables 1 and 2, respectively. The atomic positions for Al and O in the spinel block were in accordance with the reported values of potassium-rich β-alumina-doped Mg.[22,26] The occupancy of Eu and Mg was 0.0882 and 0.526, respectively. The result for the Eu content, substituting into Ba sites on the mirror plane, matches the values reported by Stevels.[21]

In addition, we calculated the maximum electron energy density (MEED) to reveal the overall structural changes in $BaMgAl_{10}O_{17}$ and $BaMgAl_{10}O_{17}$:Eu^{2+} using the MEM method. In calculating the R factors, 60 reflections of the F-type constraint and 8 reflections of the G constraint from the best Rietveld fit in $P6_3/mmc$ were analyzed. Figure 5 shows MEM maps of the mirror plane for the BAM host lattice and 11.6 mol % Eu-doped blue phosphor. The final R factors obtained from the F_o analysis of the X-ray powder reflections are $R_F = 1.76\%$ and $wR_F = 1.64\%$ for the BAM host lattice, and $R_F = 1.66\%$ and $wR_F = 1.53\%$ for the BAM blue phosphors. To see the arrangement of atoms, we calculated the electron density contour map projected from $z = 0$ to $z = {}^1/_4$ obtained by MEM. In the contour map, one-quarter of a unit cell, which contains one spinel block and one mirror plane, is projected onto the (001) plane. As shown in Figure 6, the MEM maps clearly show the significant difference in the electron density attributable to the Ba

(24) Oshima, S.; Kitamura, K.; Shigeta, T.; Horii, S.; Matsuoka, T.; Tanaka, S.; Kobayashi, H. *J. Electrochem. Soc.* **1999**, *146*, 392.

(25) Ronda, C. R.; Smets, B. M. J. *J. Electrochem. Soc.* **1989**, *136*, 570.

(26) Iyi, N.; Inoue, Z.; Kimura, S. *J. Solid State Chem.* **1986**, *61*, 236.

Table 1. Crystallographic Data of $BaMgAl_{10}O_{17}:Eu^{2+}$ (11.6 mol % Eu)[a]

atom	site[b]	g[c]	x	y	z	$U_{iso} \times 100$[d] (Å^2)
Ba(1)	2d	0.9118	0.3333(3)	0.6666(7)	0.75	1.01(1)
Eu(1)	2d	0.0882	0.3333(3)	0.6666(7)	0.75	1.23(2)
Al(1)	12k	1.0	0.1660(8)	0.3321(6)	-0.1058(1)	0.45(3)
Al(2)	4f	0.474	0.3333(3)	0.6666(7)	0.0238(5)	0.06(7)
Mg(1)	4f	0.526	0.3333(3)	0.6666(7)	0.0238(5)	0.06(7)
Al(3)	4f	1.0	0.3333(3)	0.6666(7)	0.1743(9)	0.34(9)
Al(4)	2a	1.0	0.0	0.0	0.0	0.25(9)
O(1)	12k	1.0	0.1543(8)	0.3087(6)	0.0516(7)	0.44(0)
O(2)	12k	1.0	0.5041(0)	1.0081(9)	0.1486(0)	0.25(5)
O(3)	4f	1.0	0.3333(3)	0.6666(7)	-0.0588(0)	0.09(9)
O(4)	4e	1.0	0.0	0.0	0.1441(8)	0.04(3)
O(5)	2c	1.0	0.3333(3)	0.6666(7)	0.25	0.73(1)

space group	$P6_3/mmc$	
lattice parameters	$a = b = 5.6268(7)$ Å	$c = 22.6620(2)$ Å
reliable factors	$R_{wp} = 12.02\%$	$R_p = 8.34\%$
	$S = 1.34\%$	

[a] Notes. Constraints on occupancy: Ba(1) + Eu(1) = 1.0; Al(2) + Mg(1)=1.0. [b] Multiplicity and Wyckoff notation. [c] Occupation factor. [d] Isotropic temperature factor.

Table 2. Selected Interatomic Distances and Bond Angles for $BaMgAl_{10}O_{17}:Eu^{2+}$(11.6 mol % Eu) Blue Phosphor at Room Temperature

	number of bonds	distance (Å)		bond angle (deg)
Tetrahedral Coordination			Tetrahedral Coordination	
M(2)[a]−O(3)	1	1.874(5)	O(1)−M(2)−O(3)	110.2(1)
M(2)−O(1)	3	1.854(2)	O(1)−M(2)−O(1)	108.7(1)
Al(3)−O(5)	1	1.713(5)	O(2)−Al(3)−O(5)	109.8(2)
Al(3)−O(2)	3	1.763(7)	O(2)−Al(3)−O(2)	109.2(2)
Octahedral Coordination			Octahedral Coordination	
Al(1)−O(3)	1	1.955(2)	O(4)−Al(1)−O(1)	84.8(2)
Al(1)−O(4)	1	1.837(4)	O(4)−Al(1)−O(2)	98.8(1)
Al(1)−O(1)	2	1.979(3)	O(3)−Al(1)−O(1)	91.7(1)
Al(1)−O(2)	2	1.879(3)	O(3)−Al(1)−O(2)	84.3(1)
Al(4)−O(1)	6	1.896(4)	O(1)−Al(1)−O(1)	81.9(2)
			O(1)−Al(1)−O(2)	92.2(7)
9-Coordinated Polyhedron			O(2)−Al(1)−O(2)	93.5(2)
M(1)[b]−O(5)	3	3.248(1)[c]	O(1)−Al(4)−O(1)	93.8(8)
M(1)−O(2)	6	2.791(1)[c]	O(1)−Al(4)−O(1)	86.2(8)

[a] M(2): Al(2) or Mg. [b] M(1): Ba or Eu. [c] Average value.

for 2d and oxygen ions for 12k in the mirror plane of β-alumina. In the case of undoped BAM lattice structure, three oxygen atoms are composed of tetrahedral symmetry with aluminum, but no contour lines link between the oxygen groups and the Ba atom. Moreover, the electron density distribution around the O atoms increases slightly as the Eu^{2+} content increases toward the critical concentration. Across the basal mirror planes the two spinel blocks are joined by an Al−O−Al column. This implies that two Eu atoms could seek a perfect structure to compensate charge neutrality in BR sites ($^2/_3$, $^1/_3$, $^3/_4$). The BR position is in the center of a trigonal prism formed by the nearest neighbor oxygen atoms, about 2.791 Å away. These are part of the nearest layers of closed-packed oxygen ions of the spinel blocks above and below the mirror plane. In addition, there are three nearest oxygen neighbors, at a distance of 3.248 Å, consisting of the column oxygen atoms, in the basal mirror plane. Note that there is virtually no electron density at the (0, 0, $^1/_4$) a-BR site or the ($^5/_6$, $^1/_6$, $^1/_4$) mO site.

Luminescence Properties. Figure 7 shows the luminescence and the excitation spectra of BAM measured at room temperature. The 254-nm excitation produces a very strong emission band peaking at 450 nm. The intensity of this blue luminescence is very dependent on the concentration of europium dopant.

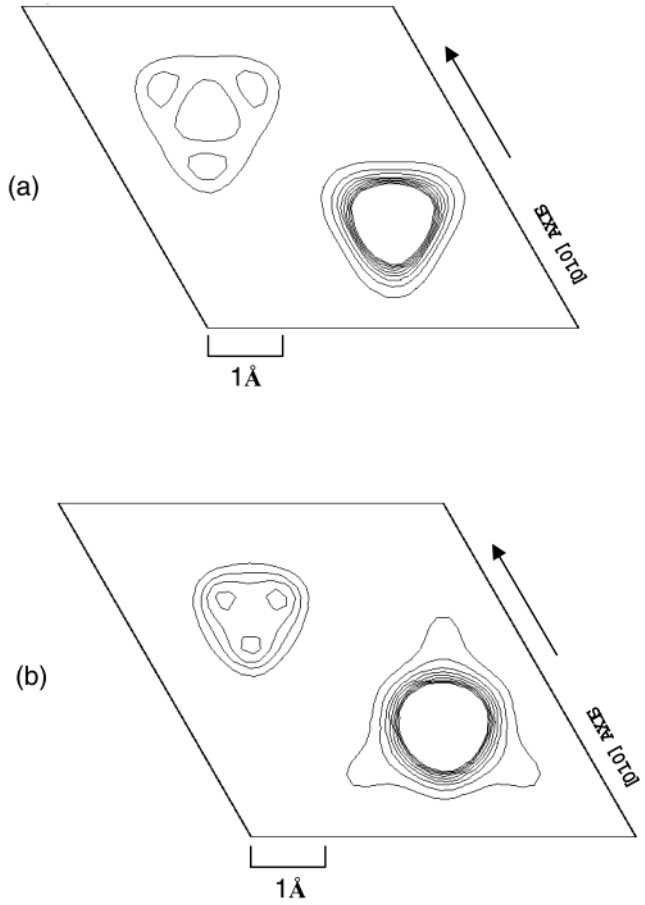

Figure 5. MEM contour maps at section $z = 0.25$: (a) $BaMgAl_{10}O_{17}$ host lattice and (b) $BaMgAl_{10}O_{17}$ doped with 11.6 mol % Eu.

With increasing Eu concentration, the intensity of the blue emission increases and reaches a maximum at a 11.6 mol %. Above this concentration, the intensity of the blue emission decreases. Additional bands on the low-energy side, responsible for the aggregation of Eu^{2+} color centers, were not found at BAM doped with high concentrations of Eu. Like the luminescence, the maximum intensity in the excitation spectrum is produced at 11.6 mol %. The typical absorption spectrum of Eu^{2+} is attributed to transitions from the $4f^7$ ground state to the highest excited state. The interaction between the

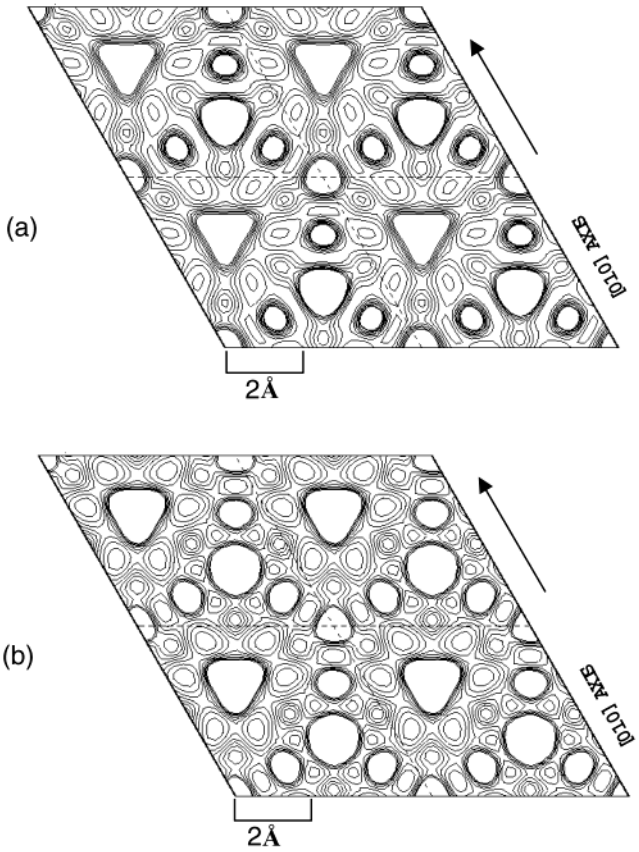

Figure 6. Projections of MEM maps from $z = 0.0$ to $z = 0.25$: (a) $BaMgAl_{10}O_{17}$ host lattice and (b) $BaMgAl_{10}O_{17}$ doped with 11.6 mol % Eu.

$4f^6$ electrons and the 5d electron is weak, so the composite $4f^65d$ system is expected to retain the nature of the uncoupled $4f^6$ and 5d states. Of the three observed excitation bands, the two low-energy bands, peaking at 254 and 310 nm, are typical transitions from the ground state to the split 5d levels of Eu^{2+}, while the 170-nm band corresponds to the excitation of the host lattice.[27] Above about 175 nm, with decreasing wavelength, the penetration depth of VUV radiation rapidly decreases because of a large absorption coefficient in fundamental absorption. It suggests that only Eu^{2+} activators on the surface of host $BaMgAl_{10}O_{17}$ may contribute to the visible emission.

Previously, the quantum efficiency of BAM has been measured by conventional methods using a standard material of well-known quantum efficiency. It was found that the quantum efficiency is ≈70% for BAM containing 2 mol % Eu and ≈60% for those containing 40 mol % Eu.[21,28] It was found that the quantum efficiency has been slightly dependent on the Eu^{2+} concentration. In this study, we measured the absolute value of the PL quantum efficiency, *Q*, of several BAMs at room temperature. This is a more accurate and practical method than the indirect method using a standard material. In Figure 8, we plot *Q* vs Eu concentration. BAM containing 4.0 mol % Eu converts only 66% of the absorbed photons to luminescence. As with the luminescence

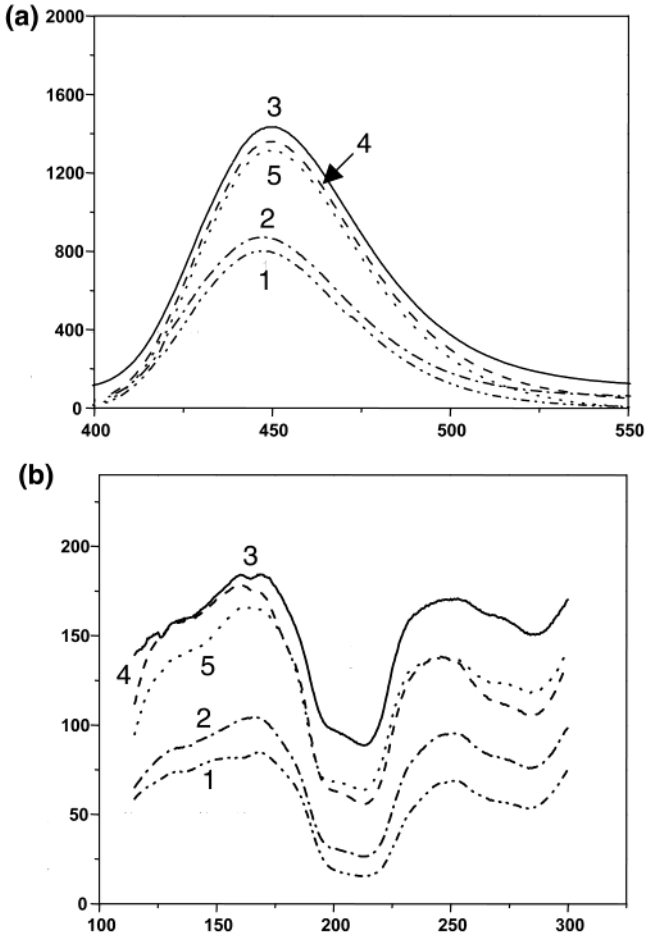

Figure 7. Eu concentration dependencies of the luminescence and excitation spectra of $BaMgAl_{10}O_{17}:Eu^{2+}$: (a) luminescence spectra (λ_{exc} = VUV) and (b) excitation spectra (λ_{exc} = 450 nm) (1, 2.3; 2, 5.3; 3, 11.6; 4, 15.8; 5, 15.8 mol %).

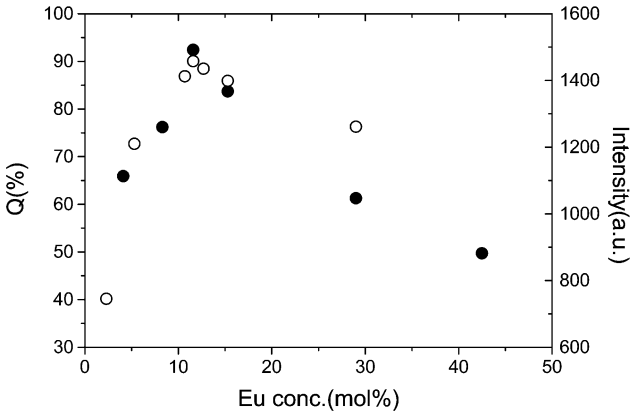

Figure 8. Eu concentration dependencies of the quantum efficiency (●) and luminescence intensity (○) of the blue emission from $BaMgAl_{10}O_{17}:Eu^{2+}$.

intensity, as the concentration of Eu ions increases, *Q* increases and reaches a maximum of $Q = 92.4\%$ for BAM containing 11.6 mol % Eu. As the concentration increases further, *Q* decreases and is only 49.7% at 42.5 mol % Eu. The concentration dependence of the luminescence intensity is also illustrated in Figure 8. The concentration dependencies of both the quantum efficiency and the luminescence intensity indicate that the Eu concentration resulting in the maximum luminescence is 11.6 mol %. This critical concentration is

(27) Poort, S. H. M.; Blokpoel, W. P.; Blasse, G. *Chem. Mater.* **1995**, *7*, 1547.
(28) Stevels, A. L. N.; Schrama-de Pauw, A. D. M. *J. Electrochem. Soc.* **1976**, *123*, 691.

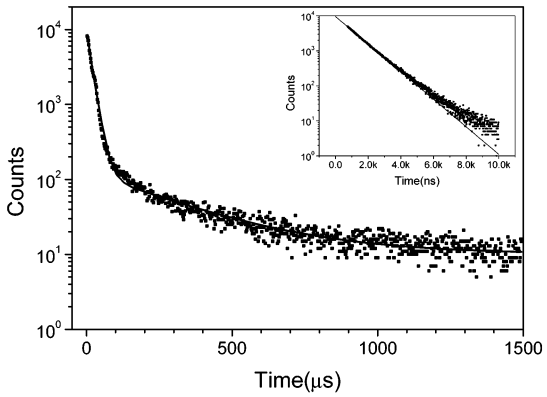

Figure 9. Typical example of the best fit of the slow and the fast (inserted) decay-time components of the 450-nm emission from $BaMgAl_{10}O_{17}:Eu^{2+}$. The solid lines show the calculated values based on two exponentials for the slow decay and a single-exponential term for the fast decay.

slightly lower than the value reported by Liu and Shi,[3] who found the critical concentrations of Eu^{2+} to be about 15 and 20 mol %, when using NH_4F and BaF_3, respectively, as a flux.

The decay times of the blue luminescence of BAM phosphors were measured on the microsecond scale at room temperature. A log plot of the luminescence data vs time is very useful for identifying whether it is a single component at the beginning of data analysis. As shown in Figure 9, the decay curve is complicated. After excitation, most populations decay within 100 μs, but there is a tail that persists for up to 1 ms. This indicates that the blue emission from Eu^{2+} can be resolved into two exponential terms. To obtain the fast decay time, we collected decay data on the nanosecond scale using a Ti-sapphier laser as a light source. A log plot of the fast decay data vs time is inserted in Figure 9. Early on, the observed data agree well with a single-exponential decay, while after 5 μs the observed decay data deviate from the solid line representing the decay time calculated using a single-exponential term. Significantly, the decay time of the blue emission from BAM consists of three components, that is, one fast and two slow decay times. We measured these three decay times for six BAM phosphors containing europium from 4.0 to 42.5 mol %. Independent of the Eu concentration, all six BAM phosphors have the fast decay times of 1.03 ($\pm$0.03) μs and the two slow decay times of 18.0 ($\pm$4.3) and 240 ($\pm$53) μs. The fast decay component contributes more than 98% of the blue emission from BAM.

Energy Transfer and the Oxidation States of Eu. The concentration effect on the quantum efficiency is significantly related to the energy transfer between activator ions when the activator is excited directly. Assuming that the dipole−dipole interaction plays a key role in the energy transition between Eu^{2+} ions, the probability, P, can be expressed by[4]

$$P_{ET} = 3 \times 10^{12} \frac{P_A}{R^6 \tau_{Eu}} \frac{1}{E^4} \int f_{Eu}(E)\, F_{Eu}(E)\, dE \quad (1)$$

where P_A is the oscillator strength of the 4f $\rightarrow$ 5d transition of Eu^{2+}, R is the distance between the Eu^{2+} ions (Å), τ_{Eu} is the decay time of the luminescence (s), E is the energy transferred (eV), and the integral is the overlap between the normalized emission and excitation bands. Practically, for the BAM, it is very difficult to calculate P_A from the absorption spectrum because of its opaque state. Although the excitation and emission spectra are well-separated, we calculated the integration of the overlap between the excitation and the emission bands. At low concentration, the energy overlap is almost constant with $\approx$0.021 eV. As the concentration increases, the energy overlap increases and reaches a maximum of 0.029 eV at 11.6 mol %. As the concentration increases furthermore, the energy overlap decreases and becomes a constant of 0.023 eV. The concentration dependence of the energy overlap apparently shows that the energy transfer between two Eu^{2+} centers is most effective at the critical concentration.

Table 3. Calculated P_{factor} and the Critical Distance of the Calculated R_c Values Depend on the Concentration of Eu mol % (X) in $BaMgAl_{10}O_{17}$ Blue Phosphors[a]

X	2.3	5.3	11.6	15.8	29.0
a	5.62761	5.62681	5.62587	5.62634	5.62615
c	22.6810	22.6676	22.6620	22.6226	22.6209
V	622.0812	621.4590	621.3772	621.3075	621.1071
g[b]	0.0029	0.0162	0.0882	0.0912	0.0966
$P_{factor} \times 10^3$	14.93(3)	14.97(3)	14.98(1)	15.14(5)	15.14(9)

[a] Note: a, c, and R_c are in Å. [b] Occupation factor in Rietveld refinement method.

Instead of using the oscillator strength and the integration of the overlap, eq 1 can be rewritten in terms of the critical distance, R_c, which can be directly determined from the crystal parameters defined as

$$R_c \approx 2\left(\frac{3V}{4\pi g N}\right)^{1/3} \quad (2)$$

where g is the substituted Eu^{2+} ion fraction at which the quenching starts and N is the number of Eu^{2+} ions in the unit cell.[29] At $R = R_c$, the probability of transfer from S to A equals the probability of the radiative emission from S, that is, $P_{SA} \times \tau = 1$. Equation 1 can be expressed in terms of R_c as

$$P_{ET} = \frac{{R_c}^6}{R^6 \tau_{Eu}} \quad (3)$$

$${R_c}^6 = 3 \times 10^{12} \frac{P_A}{E^4} \int f_{Eu}(E)\, F_E(E)\, dE \quad (4)$$

Furthermore, the energy transfer between Eu^{2+} ions positioned in the different layer is different from that between Eu^{2+} ions in the same layer. When P_{factor} is defined as the ratio of the probabilities of transfer between nearest neighbors, it can be approximated by the crystal parameters as

$$P_{factor} = \frac{P(\text{different} - \text{mirror} - \text{plane})}{P(\text{same} - \text{mirror} - \text{plane})} \approx \left(\frac{a}{c/2}\right)^6 \quad (5)$$

The calculated values of P_{factor} are listed in Table 3. The ratio of the probabilities of transfer between the nearest neighbors, P_{factor}, shows that the energy transfer between Eu^{2+} ions in the same mirror plane such as $z = 0.25$ or $z = 0.75$ is much more effective than that

(29) Blasse, G. *J. Solid State Chem.* **1974**, *9*, 147.

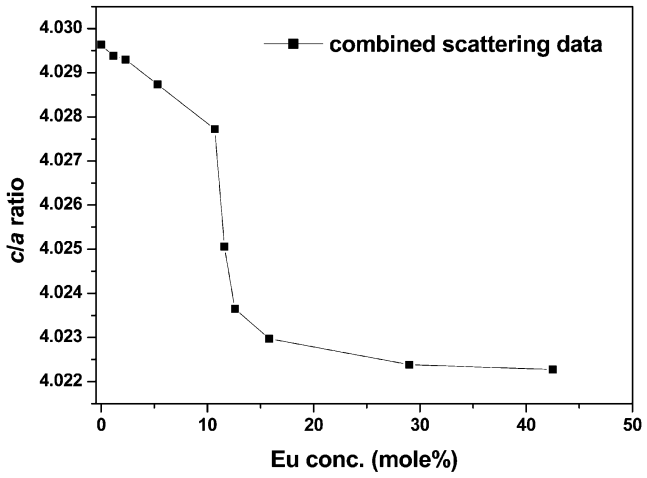

Figure 10. Plot of c/a vs the Eu concentration.

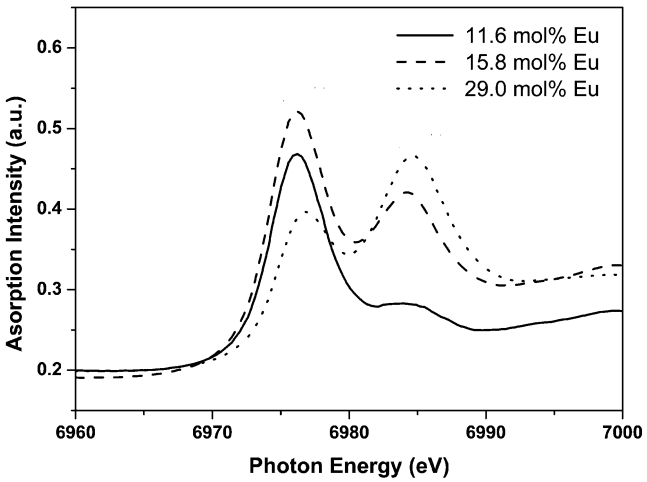

Figure 11. XANES spectra of $BaMgAl_{10}O_{17}$:Eu (L-shell of Eu atom) at various Eu concentrations.

between Eu^{2+} ions in different mirror planes across the spinel block. At the critical concentration, we found that $R_c = 18.8(7)$ Å and $P_{ET} = 1.39254 \times 10^9$ (s^{-1}) with $\tau = 1.0$ ms and $R = 5.62587$ Å.

As expressed by eq 5, the concentration dependence of P_{factor} is inversely proportional to that of the c/a ratio. As shown in Figure 10, with increasing Eu^{2+} content, the c/a ratio generally decreases to an extent, which is expected, since the ionic radius of Eu^{2+} (1.12 Å) is smaller than that of Ba^{2+} (1.34 Å). Furthermore, as the Eu^{2+} concentration increases to near the critical concentration, the c/a ratio decreases steeply. Subsequently, with increasing concentration, the ratio gradually decreases. At low concentration, Eu^{2+} ions can easily be accommodated into the Ba^{2+} site in the mirror plane of the 2d site ($^1/_3$, $^2/_3$, $^3/_4$); however, there is a limitation at that Ba^{2+} site. As the Eu^{2+} concentration increases to near the critical concentration, the solubility of the Eu^{2+} ion in the mirror plane may become saturated. It is very difficult for extra Eu^{2+} ions to substitute into the spinel block since the Mg^{2+} ions that are easily accommodated in an Al^{3+} tetrahedral site may expel the larger Eu^{2+} from the spinel block. To reveal the environmental conditions of the Eu ion, we measured X-ray absorption near-edge structure (XANES) spectra of the L-shell of Eu ions in $BaMgAl_{10}O_{17}$, using Pohang Accelator 3C1 line. As shown in Figure 11, there are two absorption bands, peaking at 6984 and 6977 eV. To identify these bands, we also measured the XANES spectrum of Eu_2O_3 oxide as a reference. Eu_2O_3 oxide produces only a 6984-eV band. Accordingly, the observed 6984- and 6977-eV bands are due to the trivalent and divalent oxidation states of europium, respectively. Note that, at 11.6 mol % of europium in $BaMgAl_{10}O_{17}$ host material, the absorption peak of Eu^{3+} at 6984 eV becomes observable. Above the critical concentration, the intensity of the 6984-eV band increases with the dopant concentration. We also measured the photoluminescence spectrum of BAM highly doped with Eu^{2+}. In the PL spectrum, nothing corresponded to the $^5D_0 \rightarrow {}^7F_J$ transitions of Eu^{3+}. These results suggest that divalent Eu atoms partially replace Ba atoms occupying the 2d site ($^1/_3$, $^2/_3$, $^3/_4$) in the mirror plane, while others may exist as the trivalent state in the unit cell. Taking into account the critical distance of 18.8 Å, the energy transfer from the luminescent centers to the defects becomes effective if the concentration exceeds the critical value. The Eu^{3+} defects, acting as radiationless sink, may be deleterious to the luminescence intensity of $BaMgAl_{10}O_{17}:Eu^{2+}$. However, it was difficult to analyze the Eu^{3+} ion quantitatively using the powder diffraction data because the X-ray scattering factor and neutron absorption effect of Eu atoms is large.

Acknowledgment. This work is partially supported by a grant (R01-2001-00055) from the Korea Science & Engineering Foundation (KOSEF). H.G.C. acknowledges financial support from KOSEF through the Research Center for Machine Parts and Materials Processing (ReMM) at the University of Ulsan. T.Y.C. acknowledges financial support from the University of Ulsan. We thank the researchers at the Pohang Accelerator Synchrotron Radiation Laboratory.

CM020592F